GENETIC INFLUENCES ON SULCAL PATTERNS OF THE BRAIN

S. H. Joshi[1], A. A. Joshi[2], B. Gutman[1], A. W. Toga[1], K. McMahon[3], G. de Zubicaray[4], N. Martin[5], M. J. Wright[5], and P. M. Thompson[1]

[1]Laboratory of Neuro Imaging, University of California, Los Angeles, USA
[2]Signal and Image Processing Institute, University of Southern California, Los Angeles, USA
[3]University of Queensland, Centre for Advanced Imaging, Brisbane, Australia
[4]University of Queensland, School of Psychology, Brisbane, Australia
[5]Queensland Institute of Medical Research, Brisbane, Australia

ABSTRACT

We present a shape-space approach for analyzing genetic influences on the shapes of the sulcal folding patterns on the cortex. Sulci are represented as continuously parameterized functions in a shape space, and shape differences between sulci are obtained via geodesics between them. The resulting statistical shape analysis framework is used not only to construct populations averages, but also used to compute meaningful correlations within and across groups of sulcal shapes. More importantly, we present a new algorithm that extends the traditional Euclidean estimate of the intra-class correlation to the geometric shape space, thereby allowing us to study heritability of sulcal shape traits for a population of 193 twin pairs. This new methodology reveals strong genetic influences on the sulcal geometry of the cortex.

Index Terms— brain imaging, sulcal curves, heritability, genetics, shape analysis

1. INTRODUCTION

The human cerebral cortex is often modeled as a highly convoluted sheet of gray matter enclosing the central white matter. Sulcal folds, or sulci are fissures in the cortical surface that are commonly used as important anatomical landmarks on the brain. These sulcal landmarks have been extensively used for cortical registration and mapping[1]. Lately, there is an emerging interest in analyzing the geometry of these patterns **[2]** for studying disease progression, brain asymmetry, development and group differences. Following this idea further, we investigate the geometry of the sulcal folds as a potentially heritable trait in human populations. Twin studies can estimate the heritability of many cognitive and behavioral traits, as well as measures derived from brain images. A typical twin study design generally involves pairs of monozygotic (MZ) and dizygotic twins (DZ). MZ twins are identical, sharing 100% of their genes, while DZ twins share on an average of 50% of the genes. Heritability studies of the brain using twins have been previously performed on anatomical features such as gray matter thickness, areas of neuroanatomical parcellations, and the volume and density of the gray matter [3]. Aside from the above phenotypes which are structural attributes of the cortex, there have been only very limited studies [4, 5, 6]attempting to investigate the heritability of the actual geometry of the sulcal folding patterns on the cortex. This is challenging because i) the sulcal patterns have to be identified in a valid and a reliable way, ii) they have to be represented efficiently and compactly, iii) there has to be a consistent morphometric framework that accurately models sulcal geometry while excluding nuisance parameters by incorporating appropriate invariances, and lastly iv) the statistical structure that is frequently used in analyzing thickness and volume cannot be directly translated to analyze features whose variation is described by nonlinear manifolds, such as shapes.

In this work, we present a mathematical framework to estimate genetic influences directly on shape of the sulcal morphology of the cortex. We will use the sulcal landmark shapes as our characteristic representations for cortical folding. First, we introduce a procedure for extracting sulcal landmark curves on the cortex (Sec. 2.1) and also outline a method for their invariant representation and analysis (Sec. 2.2). We then formulate a new extension to the method of computing intra-class correlations between shapes (Sec. 2.3), and extend it to obtain a measure of heritability. Our analysis shows that not only the anatomical tissues and morphological features in the brain are genetically influenced, but the the shape of the sulcal folding patterns show genetic influence as well.

2. MATERIALS AND METHODS

2.1. Sulcal Shape Extraction

To automatically delineate sulcal landmarks on the cortex, we use the BrainSuite software [7] to first extract the tessellated cortical surface for the atlas and each subject from T1-weighted MRI volumes and then to automatically iden-

This work was supported by NIH grant R01 HD050735, NHMRC (Australia) grant 496682, R01 EB008281, and P41 RR013642.

tify sulcal landmarks on the cortex. This method sets up an automatic one-to-one correspondence between the atlas surface and the subject surface. Furthermore the atlas surface is accompanied by 26 manually labeled and validated candidate sulcal curves according to the protocol described in [8]. By using the curvature-based point correspondence established using BrainSuite registration, these curves are then transferred to the subject surface. We also emphasize that other automated registration methods (e.g. Freesurfer, Brainvisa or Brainvoyager) could also be used to transfer the atlas sulcal curves to their corresponding locations on the subject.

2.2. Sulcal Shape Analysis Framework

The automatically extracted sulci are obtained as a set of ordered points on the cortical surface. Instead of using a landmark-based approach for shape analysis, we represent sulci using arbitrarily parameterized functions [9] as follows. For a set of 3D ordered points for a specific sulcus, we first obtain a continuous parameterization $p(s) : [0, 2\pi] \rightarrow \mathbb{R}^3$, where s is an arc-length parameter, and then represent its shape by the function $q : [0, 2\pi] \rightarrow \mathbb{R}^3$ as $q(s) = \frac{\dot{p}(s)}{\sqrt{||\dot{p}(s)||_{\mathbb{R}^3}}} \in \mathbb{R}^3$. Here, $s \in [0, 2\pi]$, $||\cdot||_{\mathbb{R}^3} \equiv \sqrt{(\cdot,\cdot)_{\mathbb{R}^3}}$, and $(\cdot,\cdot)_{\mathbb{R}^3}$ is the standard euclidean inner-product in $\mathbb{R}^3$. The quantity $||\dot{p}(s)||$ is the instantaneous "speed" of the curve, and the ratio $\frac{\dot{p}(s)}{||p(s)||_{\mathbb{R}^3}}$ is the instantaneous direction (unit vector) along the curve. To make the representation scale-invariant, we will normalize the function q by its magnitude. The original curve p can be recovered or reconstituted, up to a translation, using $p(s) = \int_0^s ||q(t)||\ q(t)\ dt$. The set of such representations is defined as the space of all scale-invariant elastic curves, and is denoted by $\mathbb{S}^q \equiv \{q | q(s) : [0, 2\pi] \rightarrow \mathbb{R}^3 | \int_0^{2\pi} (q(s), q(s))_{\mathbb{R}^3} ds = 1\}$. On account of scale invariance, the space $\mathbb{S}^q$ becomes an infinite-dimensional unit-sphere and represents all open elastic curves invariant to translation and uniform scaling. In our previous work [9], we outlined a method for comparing sulcal shapes. Since the purpose of this paper is to extend the notion of intra-class correlations to the nonlinear shape space, we state the main ideas in sulcal shape analysis here and refer the reader to [9] for details. We know that geodesics on a sphere are great circles, and For a given pair of sulcal shapes q_1 and q_2, the geodesic (shortest path) between them on the sphere is given by $\chi_t(q_1, q_2) = \cos\left(t \cos^{-1}\langle q_1, q_2\rangle\right) q_1 + \sin\left(t \cos^{-1}\langle q_1, q_2\rangle\right) f$, where $f = q_2 - \langle q_1, q_2\rangle q_1$. The geodesic shape distance is then given by $d(q_1, q_2) = \int_0^{2\pi} \sqrt{\langle \dot{\chi}_t, \dot{\chi}_t\rangle} dt$. Additionally, we would like the geodesics to be invariant to rotations, and since we are dealing with parameterized curves, we would like the geodesic to be invariant to reparameterizations (denoted by the function γ) which are monotonically increasing and differentiable, nonlinear functions that change the speed of the curve. Joshi et al. [9] then define a reparameterization invariant geodesic as $d_e(q_1, q_2) = \text{argmin}_{O \in SO(2), \gamma}\, d(q_1, O(\sqrt{\dot{\gamma}} q(\gamma)))$ and also provide the algorithm for its computation. Finally given a population of sulcal shapes $\{q_i\}, i = 1, \ldots, N$, their intrinsic mean shape is defined as

$$\mu = \underset{q_\mu}{\text{argmin}} \sum_{i=1}^{N} d_e(q_\mu, q_i)^2, i = 1, \ldots, N. \qquad (1)$$

This intrinsic mean shape is fully invariant to rotations, scaling and reparameterizations. We emphasize that it is this invariance to reparameterization that motivates the refinement of the standard intra-class correlation algorithm when applied to sulcal geometries in shape spaces.

2.3. Intra class correlations (ICC) between sulcal shapes

Since the space of sulcal shapes is non-linear, one cannot directly compute the intra class correlations (ICC) [10] between shapes using standard euclidean means and variances. Therefore, we propose a new algorithm for computing ICC based on the previously described nonlinear matching between sulcal shapes. This modified ICC accepts pairs of sulcal shapes as input targets and calculates the intra-class correlations between them. For N pairs of target shapes, we denote $\{\beta_i^j\}$ as the native sulcal curves for pair i, and pair-individual j, where $i = 1, \ldots, N, j = 1, \ldots, k$. Let $\{q_i^j\}$ be the shape representations for $\{\beta_i^j\}$, and $\{p_{\beta_i^j}\}$be the reconstituted curves from $\{q_i^j\}$. We denote all the k shapes for the i^{th} target as $\{q_i\}$, and all the Nshapes for the j^{th} rater as $\{q^j\}$. Furthermore we assume the parameterization function as $s \in [0, 2\pi]$.

3. RESULTS

We demonstrate our method on a set of paired data consisting of both monozygotic (MZ) and dizygotic (DZ) twins, and compute the intra-class correlations within both pairs using Algorithm 1.

3.1. Data

Our data consisted of 3D structural brain MRI scans of 386 normal, right-handed subjects (age range: 22-25 years). The scans were collected using a 4 Tesla Bruker Medspec whole body scanner (Bruker Medical, Ettlingen, Germany) at the Center for Magnetic Resonance (University of Queensland, Australia). Three-dimensional T1-weighted images were acquired with a magnetization prepared rapid gradient echo (MP-RAGE) sequence to resolve anatomy at high resolution. Acquisition parameters were: inversion time (TI) /repetition time (TR) /echo time (TE) = 1500 / 2500 / 3.83 msec.; flip angle = 15 degree; slice thickness = 0.9mm with a 256 × 256 × 256 acquisition matrix. Specifically the data consisted of 120 MZ, and 73 DZ twin pairs. This data was processed using

Algorithm 1: Intra class correlation (ICC) for paired target shapes of curves.

Compute the mean shape of all curves $\{q_i^j\}$ and denote it as $\mu_{tot} = \text{argmin}_{q_\mu} \sum_{i=1}^{N} \sum_{j=1}^{k} d_e(q_\mu, q_i^j)^2$. Obtain the reconstituted mean curve as $p_{\mu_{tot}}$.

for $i = 1, \ldots, N$ *targets* **do**

  Compute $\mu_{q_i} = \mu(\{q_i\}) = \text{argmin}_{q_\mu} \sum_{j=1}^{k} d_e(q_\mu, q_i^j)^2$ according to Eqn. 1.

  Compute the geodesic from μ_{q_i} to q_i, and find the optimal reparameterization $\hat{\gamma}_i = \text{argmin}_\gamma [d_e(\mu_{q_i}, q_i \cdot \gamma)]$.

  Obtain the reconstituted curves $p_{\mu_{q_i}}$, and p_{q_i} using the

  Compute the geodesic from μ_{tot} to q_i and find the optimal reparameterization $\hat{\gamma}_{tot_i} = \text{argmin}_\gamma [d_e(\mu_{tot}, q_i \cdot \gamma)]$.

end

$WSS(s) = \sum_{i=1}^{N} ||p_{\mu_{q_i}} - p_{q_i}(\hat{\gamma}_i)||^2, s \in [0, 2\pi]$.

$WMS(s) = \frac{WSS(s)}{N(k-1)}, s \in [0, 2\pi]$.

for $j = 1, \ldots, k$ *raters* **do**

  Compute $\mu_{q^j} = \mu(\{q^j\}) = \text{argmin}_{q_\mu} \sum_{i=1}^{N} d_e(q_\mu, q_i^j)^2$ according to Eqn. 1.

  Compute the geodesic from μ_{tot} to μ_{q^j}, and find the optimal reparameterization $\hat{\gamma}^j = \text{argmin}_\gamma [d_e(\mu_{tot}, \mu_{q^j} \cdot \gamma)]$.

  Obtain the reconstituted curve $p_{\mu_{q^j}}$ using Eqn. XX.

end

$RSS(s) = \sum_{j=1}^{k} ||p_{\mu_{tot}} - p_{q^j}(\hat{\gamma^j})||^2, s \in [0, 2\pi]$.

$RMS(s) = \frac{RSS(s)\ N}{k-1}, s \in [0, 2\pi]$.

$BSS(s) = \sum_{i=1}^{N} ||p_{\mu_{tot}} - p_{q_i}(\hat{\gamma}_{tot_i})||^2, s \in [0, 2\pi]$

$BMS(s) = \frac{BSS(s)\ k}{N-1}, s \in [0, 2\pi]$

$ESS(s) = WSS(s) - RSS(s)$

$EMS(s) = \frac{ESS(s)}{(k-1)(N-1)}$

$ICC(s) = \frac{BMS(s) - EMS(s)}{BMS(s) + (k-1)EMS(s)}$

the BrainSuite automated processing pipeline [7] and underwent automatic skull stripping, tissue classification, surface extraction, gray matter thickness estimation and cortical and subcortical parcellation of the data.

3.2. Intra-class correlations within twin-pairs for MZ (rMZ)

The main advantage of using the twin-paired data is that it allows us to estimate the proportion of the observed variance in a trait that is attributable to genetic as well as environmental factors. Since in this paper, our trait of interest is the morphology of the sulcal patterns on the cortex, we measured differences in sulcal shapes using the matching framework outlined in Sec. 2.2. We used Algorithm 1 for computing the intra-class correlations for MZ ($N = 120$), and DZ ($N = 73$) pairs. In this study, we excluded non-paired subjects, hence for the purpose of computing ICC, we set $k = 2$. Algorithm 1 calculates within-pair and across-pair sum squared-errors at each point of the sulcus. In order to evaluate the effectiveness of elastic sulcal matching in computing the intra-class correlations, we compared the values of rMZ using both the conventional linear matching approach as well as our elastic matching approach. In case of linear matching we set $\hat{\gamma}(s) = s, \forall s \in [0, 2\pi]$, whereas we estimate an optimal reparameterization or matching function in the case of elastic matching at every step of Algorithm 1. It is observed that one could have computed rMZ using the traditional Euclidean approach directly from the point landmarks of the sulci similar to Lohmann et al. [4], but to be consistent with our comparisons, we provide an initial advantage to the method of linear matching by parameterizing the sulcal curves, and projecting them in the shape space thus making them invariant to translation, scaling, and rotation. Figure 1 shows the computation of rMZ for both the hemispheres for linear as well as elastic matching. It is seen that in general everywhere across the sulci, the rMZ values in the case of elastic matching are higher than linear matching.

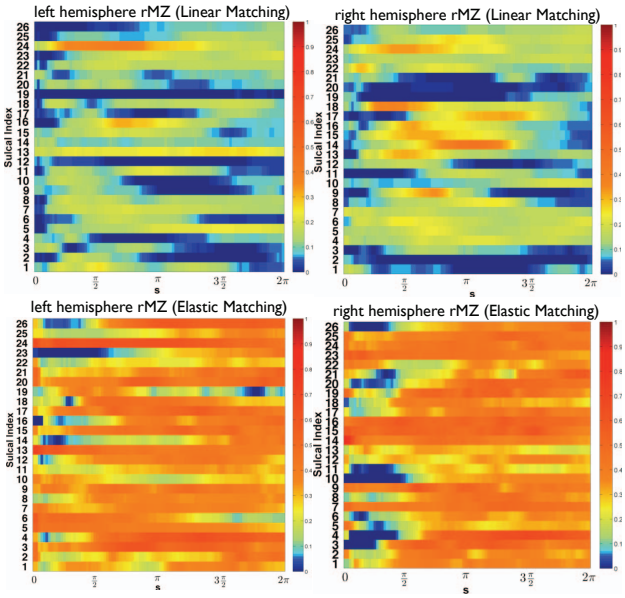


Fig. 1. Comparison of intra-class correlations (rMZ) between linear and elastic sulcal matching for monozygotic twins. $rMZ$is displayed for each sulcus type (row-wise) along its length (column-wise) for both the hemispheres.

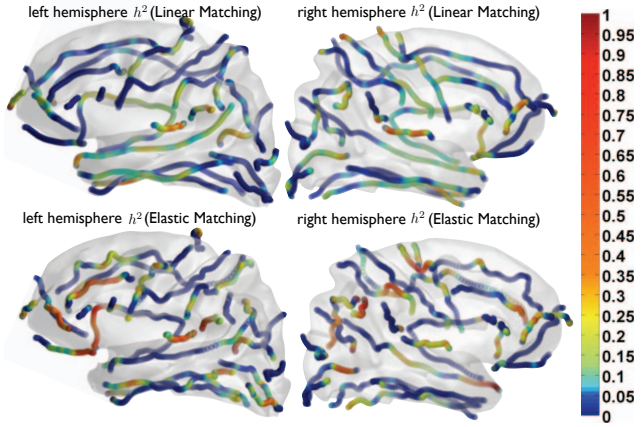


Fig. 2. Comparison of the heritability between linear and elastic sulcal matching. Color coded values of h^2 are overlaid on each sulcal population average curve.

3.3. Falconer's Estimate of Heritability (h^2)

Finally, we present results of the heritability analysis using the Falconer's estimate [11] for our twin data. Falconer's estimate estimates the broad sense heritability by measuring the difference between the monozygotic and dizygotic correlations and is given by $h^2 = 2(rMZ - rDZ)$. Figure 2 shows the comparison of h^2 for both the linear and elastic sulcal matching overlaid on the shape averages of the sulci under both methods . Clearly, when sulci are elastically matched, the heritability estimate is considerably higher (mean $h^2 > 0.4$ or higher) in the left hemisphere for the inferior frontal sulcus, lateral orbital sulcus, fronto-marginal sulcus, medial orbital sulcus, the Sylvian fissure terminal split, inferior temporal sulcus, transverse temporal sulcus, circular sulcus, occipito-parietal sulcus, calcarine sulcus, and the lateral occipital sulcus. In case of the right hemisphere, the precentral sulcus, inferior frontal sulcus, lateral orbital sulcus (latOS), frontomarginal sulcus, cingulate sulcus, paracentral sulcus, sup. temporal (with upper branch) sulcus, transverse temporal sulcus, postcentral sulcus, intraparietal sulcus, subparietal sulcus, and the calcarine sulcus all showed an increase in heritability (mean $h^2 > 0.3$ or higher) in case of the elastic matching. Also, sulcal shape population averages that were based on the elastic matching show richer geometrical features (more shape details) compared to the smoother, flatter averages due to linear matching.

4. DISCUSSION AND CONCLUSION

We proposed a new method to calculate the intra-class correlation for sulci that uses the geodesic distance instead of Euclidean dispersion. We also used the notion of the intrinsic mean in the shape space instead of the Euclidean average. This method exploits the intrinsic geometric structure in sulcal shapes, and offers an advantage over the conventional method by optimizing over the morphometric sulcal signatures, boosting the detection of the genetic signal. The new algorithm revealed greater intra-class correlations between the monozygotic pairs compared to the conventional method and also generated increased heritability estimates. Even if there are regions with higher values of h^2 in the linear case, we note that for almost all sulci the rMZ values are much smaller than the elastic case, thus showing substantially weaker intra-class correlations. Our new algorithm is widely applicable, and can be used for general studies where one seeks to perform rater reliability analysis, even for populations not consisting of twins. Finally we underscore the main contribution of this paper, that the heritability estimates obtained using this method were exclusively computed using the geometric shape of the sulci and did not involve the prevailing heritable phenotypes such as cortical thickness and volume. From a biological point of view, these heritable sulcal shapes may also be a plausible target for genetic association studies, which aim to find common variants on the genome that relate to individual variations in brain structure.

5. REFERENCES

[1] P. Thompson and A. Toga, "A surface-based technique for warping 3-dimensional images of the brain," *IEEE Tran. Med. Imagng*, vol. 15, no. 4, pp. 402–417, 1996.

[2] G. Lohmann, D. Y. von Cramon, and A. C. F. Colchester, "Deep sulcal landmarks provide an organizing framework for human cortical folding," *Cereb Cortex*, vol. 18, no. 6, pp. 1415–1420, 2008.

[3] U. Yoon, C. Fahim, D. Perusse, and A. Evans, "Lateralized genetic and environmental influences on human brain morphology of 8-year-old twins," *Neuroimage*, vol. 53, no. 3, pp. 1117–1125, 2010.

[4] G. Lohmann, D. Von Cramon, and H. Steinmetz, "Sulcal variability of twins," *Cerebral Cortex*, vol. 9, no. 7, pp. 754–763, 1999.

[5] G. Le Goualher, A. Argenti, M. Duyme, W. Baaré, H. Hulshoff Pol, D. Boomsma, A. Zouaoui, C. Barillot, and A. Evans, "Statistical sulcal shape comparisons: application to the detection of genetic encoding of the central sulcus shape," *Neuroimage*, vol. 11, no. 5, pp. 564–574, 2000.

[6] J. Kippenhan, R. Olsen, C. Mervis, C. Morris, P. Kohn, A. Meyer-Lindenberg, and K. Berman, "Genetic contributions to human gyrification: sulcal morphometry in williams syndrome," *The Journal of neuroscience*, vol. 25, no. 34, pp. 7840–7846, 2005.

[7] D. W. Shattuck and R. M. Leahy, "Brainsuite: An automated cortical surface identification tool," *Medical Image Analysis*, vol. 8, no. 2, pp. 129–142, 2002.

[8] D. Pantazis, A. Joshi, J. Jiang, D. Shattuck, L. Bernstein, H. Damasio, and R. Leahy, "Comparison of landmark-based and automatic methods for cortical surface registration," *NeuroImage*, vol. 49, no. 3, pp. 2479–2493, 2010.

[9] S. Joshi, R. Cabeen, B. Sun, A. Joshi, B. Gutman, A. Zamanyan, S. Chakrapani, I. Dinov, R. Woods, and A. Toga, "Cortical sulcal atlas construction using a diffeomorphic mapping approach," *Medical Image Computing and Computer-Assisted Intervention–MICCAI 2010*, pp. 357–366, 2010.

[10] P. Shrout and J. Fleiss, "Intraclass correlations: uses in assessing rater reliability." *Psychological bulletin*, vol. 86, no. 2, pp. 420–428, 1979.

[11] D. Falconer, T. Mackay, and R. Frankham, "Introduction to quantitative genetics (4th edn)," *Trends in Genetics*, vol. 12, no. 7, p. 280, 1996.